RESILIENT INFRASTRUCTURE

June 1–4, 2016

RESILIENT INFRASTRUCTURE LONDON 2016

INVESTIGATION OF STABLE AND UNSTABLE FIBER-REINFORCED ELASTOMERIC ISOLATORS

Niel C. Van Engelen
Rowan Williams Davies & Irwin Inc., Guelph, Canada

Michael J. Tait
McMaster University, Hamilton, Canada

Dimitrios Konstantinidis
McMaster University, Hamilton, Canada

ABSTRACT

Fiber-reinforced elastomeric isolators (FREIs) are a potentially low-cost alternative to conventional steel-reinforced elastomeric isolators. FREIs can exhibit a non-linear horizontal force-displacement relationship characterized by a softening and stiffening phase, similar to other adaptive isolation devices such as the triple friction pendulum. This non-linear relationship is a consequence of unique deformations that occur during horizontal displacement denoted as *rollover*, which causes softening, and *full rollover*, which causes stiffening. The magnitude of the softening due to rollover is primarily governed by the width-to-total height aspect ratio of the FREI. If the aspect ratio is low, below about 2.5, the isolator may be susceptible to horizontal instability where the tangential stiffness becomes negative before increasing due to full rollover. Design codes prevent the use of an isolation system susceptible to horizontal instability within the design displacement. In this paper, experimental testing is used to calibrate a numerical model of a base isolated structure using horizontally unstable and stable FREIs. The performance of the structure is evaluated based on peak displacement of the isolation layer and peak acceleration of the base isolated structure. For the isolators considered, it is shown that the horizontal instability does not have a negative impact on the performance of the structure. It is postulated that some level of horizontal instability may be allowed in the design of unbonded FREIs.

Keywords: Fiber-reinforced; elastomeric isolators; base isolation; seismic isolation; stable unbonded

1. INTRODUCTION

Large areas of Canada are relatively seismically inactive or have low population densities with low seismic risk. Regardless, large population centers reside along the St. Lawrence River valley and the west coast of British Columbia; two of the most seismically active areas in Canada. The potential for losses due to earthquakes in these regions has been estimated to exceed 60 billion (AIR Worldwide 2013), in addition to large numbers of injuries and fatalities. The National Building Code of Canada anticipates and accepts that damage will occur within a structure, utilizing ductility in the form of plastic hinging to protect the structure from catastrophic failure. This approach does little to protect the non-structural components and systems, which can exceed 80% of the total value of the structure (Taghavi et al. 2003). Combined with the cost of repairs or demolition and reconstruction of the structure and the potential loss of functionality, this approach may have staggering economic consequences.

Each earthquake offers lessons for researchers and has fuelled the drive for the development of unique mitigation systems to address the protection of the structure and the non-structural components and systems. Amongst these innovative technologies is seismic base isolation. Seismic base isolation has been gaining popularity within the earthquake engineering community in recent decades. A comparison of a seismically base isolated structure and a conventional fixed base structure is shown in Figure 1. In a conventional fixed base structure, ground accelerations develop large accelerations and related inertial forces within the structure. In a base isolated structure, a flexible layer is introduced, usually at the foundation level, to decouple the structure from the strong ground motions. As an

earthquake occurs, the flexible layer allows large displacements to occur. The flexible layer essentially allows the structure to respond as a near-rigid block on top of the isolation system. The performance of a base isolation system is primarily related to its ability elongate the fundamental period of the structure, shifting it out of the high energy range of a typical earthquake event.

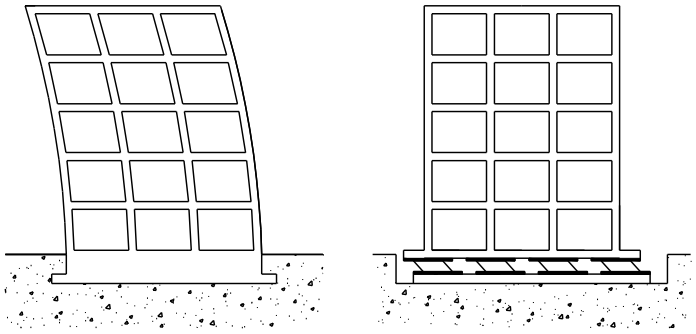

(a) (b)

Figure 1: Example of the response of (a) a fixed base and (b) a base isolated structure to strong ground motions

Elastomers are often used in seismic isolation devices due to their soft material properties and ability to undergo large recoverable strains. Elastomeric isolators can be divided into two main categories: steel-reinforced and, more recently, fiber-reinforced. A steel-reinforced elastomeric isolator (SREI) is composed of alternating horizontal layers of steel and elastomer and usually has large steel endplates used to mechanically fasten the isolator to the upper and lower supports, shown in Figure 2. The steel reinforcement stiffens the vertical properties, forming a device that is very stiff in the vertical direction, yet flexible in the horizontal direction. This is necessary to support the large weight of the structure while still allowing large horizontal displacements to occur.

Fiber-reinforced elastomeric isolators (FREIs) were initially proposed as a potential low-cost alternative to conventional SREIs (Kelly 1999). In a FREI, the steel reinforcement is removed and replaced with lighter fiber reinforcement with similar mechanical properties in tension. The steel endplates may also be removed and the isolator can be positioned unbonded between the supports, relying on friction to transfer the horizontal forces.

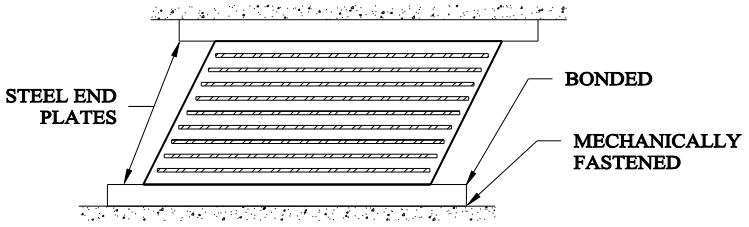

Figure 2: Typical bonded SREI or FREI under horizontal displacement

Unbonded FREIs exhibit a non-linear horizontal force displacement relationship due to unique deformations known as *rollover* and *full rollover*. The device softens as rollover occurs, and begins to stiffen as full rollover occurs. Devices that exhibit a softening and stiffening response are denoted as adaptive devices. Adaptive devices are considered advantageous for seismic isolation as the response can be tailored to the earthquake hazard level. In unbonded FREIs with low width-to-total height aspect ratios, rollover can develop a horizontal instability as the tangential stiffness becomes negative. Design codes, such as ASCE-7 (ASCE 2010), require that an isolation system retain horizontal stability (i.e. a positive tangential horizontal stiffness). In this paper, the response of a base isolated structure isolated with stable unbonded FREIs and unstable unbonded FREIs is compared. Experimental testing is used to calibrate a numerical model. The response of the structure is evaluated based on the peak displacement of the isolation layer and peak acceleration of the structure.

2. BACKGROUND

SREIs are inherently heavy and expensive (Kelly and Konstantinidis 2011). The weight and cost of this device can be perceived as barriers to widespread base isolation application, particularly in developing countries where the devastation due to earthquakes is often more severe. Consequently, base isolation has thus far been largely exclusive to high importance structures and post disaster buildings (Kelly and Konstantinidis 2011). FREIs were initially proposed as a potentially low-cost alternative to conventional SREIs (Kelly 1999). The concept focused on developing a lighter device that could achieve similar performance as a conventional SREI. In addition to replacing the steel reinforcement with lighter fiber reinforcement, the large steel end plates were removed in favour of an unbonded application to simplify installation and further reduce the weight.

The installation of the device in an unbonded application lead to advantageous performance features (Toopchi-Nezhad et al. 2008). As an unbonded FREI is displaced horizontally, the initially vertical faces of the isolator rotate and the isolator begins to lose contact with the upper and lower supports. This deformation, shown in Figure 3a, is denoted as *rollover*. Rollover is a consequence of the unbonded application and the lack of flexural rigidity of the fiber reinforcement. The resistance to horizontal displacement is less in the volume of elastomer that has experienced rollover (i.e. lost contact with the supports) than an equivalent volume in simple shear (Van Engelen et al. 2014, Russo et al. 2013, Kelly and Konstantinidis 2007). Thus, as the isolator is displaced horizontally and the size of the rollover section increases, the isolator softens. The softening due to rollover continues until the initially vertical faces rotate 90 degrees and contact the upper and lower supports, completing *full rollover*, as shown in Figure 3b. The occurrence of full rollover prevents additional rollover and the horizontal force-displacement relationship begins to stiffen. Note that the dependency of this device on friction to transfer the horizontal forces determines that it is susceptible to slip and permanent deformations in certain extreme earthquake events, and is unable to resist any tensile loads. These limitations were identified and addressed in Van Engelen et al. (2015a), which proposed a hybrid between a bonded isolator and an unbonded isolator. Unbonded FREIs have been experimentally investigated with average vertical stresses up to 18 MPa (de Raaf et al. 2011).

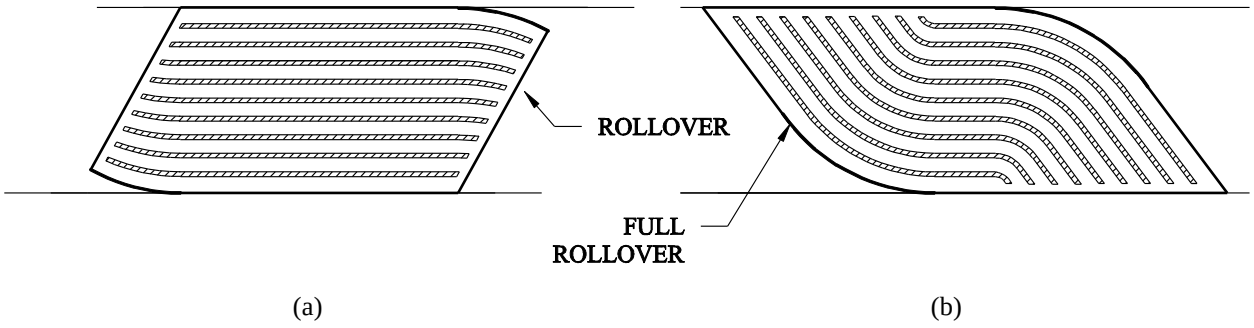

Figure 3: Deformed shape of an unbonded FREI a horizontal displacements showing (a) rollover and (b) full rollover

Rollover and full rollover are the characteristic features of unbonded FREIs. Seismic isolation devices that exhibit a softening and stiffening response, such as the triple friction pendulum and sliding devices with variable curvature, are considered to be adaptive devices (Fenz and Constantinou 2008, Tsai et al. 2003). Adaptive devices have a large initial stiffness to prevent excessive displacements during low service loading events. As larger events occur (e.g. design basis earthquake (DBE)), the device begins to soften, which increases the efficiency of the device due to a larger shift in the fundamental period. During very large events (e.g. the maximum considered earthquake (MCE)), the device begins to stiffen, which is believed to act as a self-restraint against excessive displacements (Van Engelen et al. 2015b).

Design codes (e.g. ASCE-7 (ASCE 2010)) require that the isolation system retain a positive tangential stiffness through all levels of imposed horizontal displacement (i.e. that the device remains horizontally stable). Unbonded FREIs are prone to horizontal instability with low width-to-total height aspect ratios (Van Engelen et al. 2014). A low aspect ratio determines that the volume of rollover becomes large in comparison to the total volume of the isolator. Thus, the magnitude of the softening exceeds the incremental force contribution of the remaining volume of elastomer and the tangential stiffness becomes negative as a consequence. The transition between an unstable and

stable FREI occurs at an aspect ratio of approximately 2.5 (Toopchi-Nezhad et al. 2008, Van Engelen et al. 2014). The response of a base isolated structure with stable unbonded FREIs has been investigated experimentally and numerically (Toopchi-Nezhad et al. 2009a,b); however, the response of a base isolated structure with unstable FREIs that experience full rollover has not been considered.

3. EXPERIMENTAL PROGRAM

Two unbonded FREI quarter scale specimens were considered in this program. The specimens were comprised of seven layers of natural rubber. The total height of the specimens was 20 mm and the total thickness of the elastomeric layers, t_r, was 19 mm. The specimens were reinforced with plain weave bi-directional carbon fiber. Both specimens were cut from the same pad with a length of 42 mm (perpendicular to the direction of testing). The width (parallel to the direction of testing) of specimen B1 was 40 mm, and the width of specimen B2 was 80 mm. Thus, the isolators had an aspect ratio of 2.0 and 4.0, respectively.

The experimental tests were conducted with vertical load control and horizontal displacement control. A photograph of the experimental apparatus is shown in Figure 4. Each specimen was placed unbonded into the apparatus and monotonically loaded to a design average vertical stress of 2.0 MPa. Three horizontal sinusoidal cycles were conducted at each of seven displacement amplitudes in ascending order: 0.25, 0.50, 0.75, 1.00, 1.50, 2.00 and 2.50 t_r. The specimen was then monotonically unloaded, removed from the apparatus and inspected for damage. The horizontal load and displacement were monitored with a single load cell and string potentiometer, respectively.

The third cycle of the horizontal force-displacement hysteresis loops are compared in Figure 5, where the horizontal force, F, has been normalized by the plan area, A, and shear modulus of the natural rubber, G, and the horizontal displacement, u, has been normalized by the total thickness of the elastomeric layers. The tangential stiffness of isolator B1 became zero at approximately u/t_r = 0.75, and horizontally unstable over the u/t_r = 1.50 cycle. Full rollover is theoretically expected to occur at u/t_r = 1.75 for this isolator design (Kelly and Konstantinidis 2007), and was observed in both isolators over the u/t_r = 2.00 cycle. Full rollover increased the horizontal stiffness and returned isolator B1 to local horizontal stability as the tangential stiffness became positive. The equivalent viscous damping, calculated from the experimental hysteresis loops, ranged between 6.3 and 10.5 % and 4.3 to 7.0 % for isolator B1 and B2, respectively.

Figure 4: Experimental apparatus

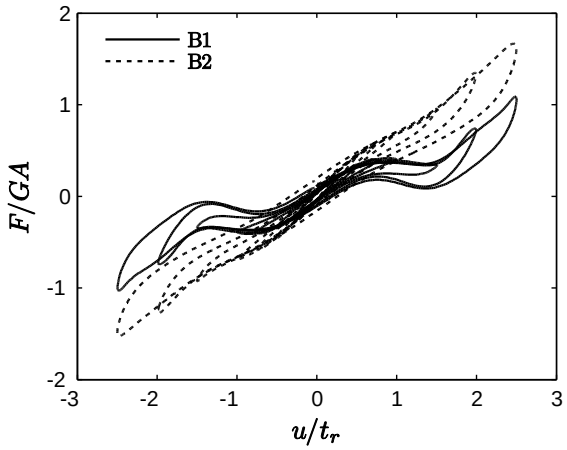

Figure 5: Comparison of the normalized experimental force-displacement hysteresis loops

4. MODEL AND METHODOLOGY

4.1 Structure

The numerical analysis was conducted using OpenSees (OpenSees 2013) in two dimensions. The single bay, two storey prototype planar frame was selected from a previous numerical investigation on unbonded FREIs (Van Engelen et al. 2015b). The total weight of the planar frame was distributed equally over the six nodes of the frame, including the isolation layer. The total weight of the frame is equivalent to the 2.0 MPa vertical stress applied in the experimental program. The beams and columns were represented using elastic beam column elements and were assumed to be axially rigid. The inherent damping of the structure was assumed to be 2 % and was applied to the structure using initial stiffness proportional damping. The fixed-base fundamental period of the full scale model was determined to be 0.21 s. The analysis was conducted in quarter scale consistent with the experimental results and planar frame; all the results are presented in full scale. Only the horizontal component of the ground motion was considered, and vertical motion was prevented at the isolation layer.

4.2 Unbonded FREIs

Love et al. (2011) numerically modelled a base isolated structure with stable unbonded FREIs calibrated from experimental results. The unbonded FREIs were represented by adapting a Bouc-Wen model with a fifth order polynomial to better represent the softening and stiffening due to rollover and full rollover. The model used herein is derived from the traditional Bouc-Wen model, as presented in Van Engelen et al. (2015b), with the inclusion of a fifth order polynomial. Accordingly, the restoring force is:

[1] $$F = a_1 u + a_2 |u| u + a_3 u^3 + a_4 |u| u^3 + a_5 u^5 + Bz$$

with

[2] $$\dot{z} = \frac{\dot{u}}{Y}\left\{\alpha - \left[\beta \operatorname{sgn}(z\dot{u}) + \gamma\right]|z|^n\right\}$$

where α, β, γ, Y, B, a_1 through a_5 and n are quantities that control the shape of the hysteresis, sgn is the sign function, and z is the hysteretic parameter. Note that this model assumes hysteretic damping, although it could be adapted to include viscous damping as well by including a viscous damping term in Eq. (1).

The numerical model was calibrated using a best-fit procedure, minimizing the squared residuals over the third cycle of the experimental results for each isolator. The force-displacement relationship of isolator B1 was multiplied by two to account for difference in loading area (i.e., two unstable isolators, B1, or one stable isolator, B2, supported each column). Figure 6 compares the experimental and model hysteresis loops.

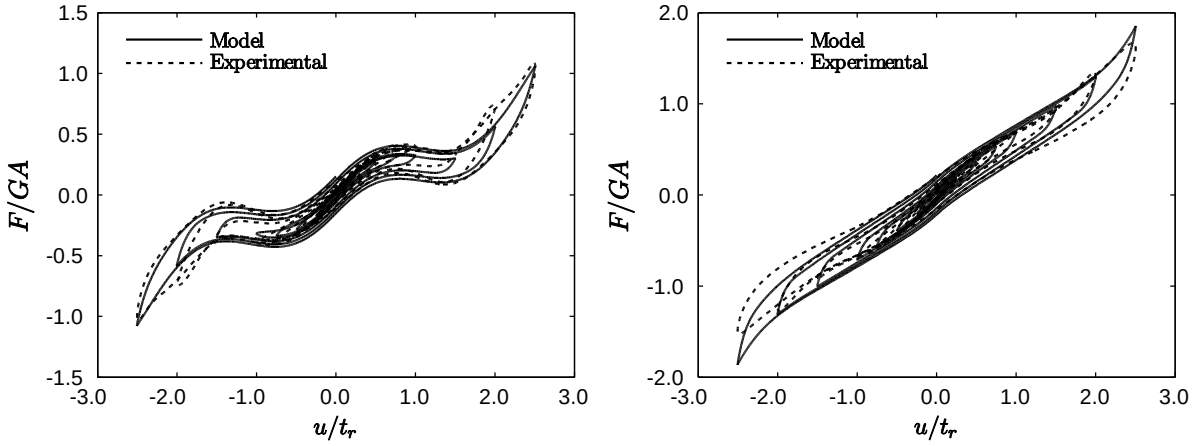

(a) (b)

Figure 6: Comparison of the model and experimental hysteresis loops for (a) isolator B1 and (b) isolator B2

4.3 Earthquakes and Scaling

The response of the base isolated structure was evaluated based on 7 fault-normal broadband ground motions on rock (Baker et al. 2011). The ground motions were scaled to a design spectrum (ASCE 2010) for Victoria City Hall, British Columbia, assuming cite class C and a 2 % probability of exceedance over 50 years (NBCC 2010). Each record was scaled to minimize the squared residuals over $0.5T_M$ to $1.25T_M$, where T_M = 1.4 s is the effective period at the MCE hazard level determined according to ASCE-7 (ASCE 2010) using the third cycles of isolator B2. Linear interpolation was applied between displacement amplitudes. The ground motions and scaling factors are shown in Table 1 and the pseudo-acceleration, S_a, response spectra is shown in Figure 7.

In the analysis, hazard levels ranging from the service level earthquake (SLE) to 1.2 MCE were considered. Increment of 0.2 MCE were considered between these levels. The relationship between the SLE, DBE and MCE was established as SLE = 1/3 MCE and DBE = 2/3 MCE.

Table 1: Selected earthquake time histories and scale factors

Earthquake	Station	Scale Factor
Loma Prieta - 1989	Gilroy Array #6	1.87
Hector Mine - 1999	Hector	0.91
Coyote Lake - 1979	Gilroy Array #6	0.70
Northridge-01 - 1994	Pacoima Dam (downstr)	1.17
Chi-Chi, Taiwan - 1999	WNT	0.69
Loma Prieta - 1989	Gilroy Array #1	1.62
Northridge-01 - 1994	LA - Dam	0.47

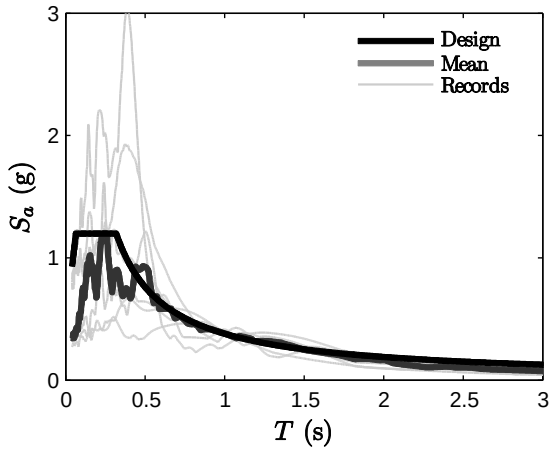

Figure 7: Pseudo-acceleration response spectrum of the selected scaled earthquake records

5. RESULTS

The normalized mean peak isolator displacement, u_{max}/t_r, and peak floor acceleration at the roof of the structure, PFA_3, are shown in Figure 8 as a function of the hazard level. The value of u_{max}/t_r for isolator B1 is initially larger than isolator B2. This is primarily due to the lower effective horizontal stiffness of isolator B1, particularly at these low horizontal displacements. This results in a larger shift in the fundamental period, which requires larger values of u_{max}/t_r. At the MCE level earthquake, both isolator B1 and B2 have an approximately equal value of u_{max}/t_r = 1.75. At this displacement amplitude, isolator B1 has entered into, and surpassed the unstable area of the hysteretic response (see Figure 5).

The ratio of the response of isolator B1 to B2 is provided in Table 2. The stiffening due to rollover observed in isolator B1 after the unstable range begins to restrain the displacement and, by 1.2 MCE, the value of u_{max}/t_r is 6 % greater in isolator B2, than B1. The relationship between u_{max}/t_r and hazard level for isolator B2 is near-linear. Note that isolator B2 had an aspect ratio of 4.0, and the magnitude of the softening (and subsequent stiffening) was small in comparison to isolator B1, resulting in a more linear force-displacement relationship. The maximum amount of softening observed in isolator B2 was 40%, compared to 70% in B1, referenced to the effective horizontal stiffness at the u/t_r = 0.25 cycle. A similar trend for isolator B2 was observed in Van Engelen et al. (2015b), which was attributed to the characteristics of the displacement response spectra.

Table 2: Numerical model results

B1		B2		B1/B2	
u_{max}/t_r	PFA_3 (g)	u_{max}/t_r	PFA_3 (g)	u_{max}/t_r	PFA_3
0.64	0.08	0.54	0.11	1.20	0.73
0.79	0.08	0.65	0.13	1.22	0.66
1.15	0.10	0.99	0.18	1.16	0.54
1.29	0.10	1.11	0.19	1.16	0.51
1.52	0.11	1.35	0.23	1.12	0.49
1.74	0.13	1.72	0.28	1.01	0.45
1.96	0.17	2.08	0.37	0.94	0.46

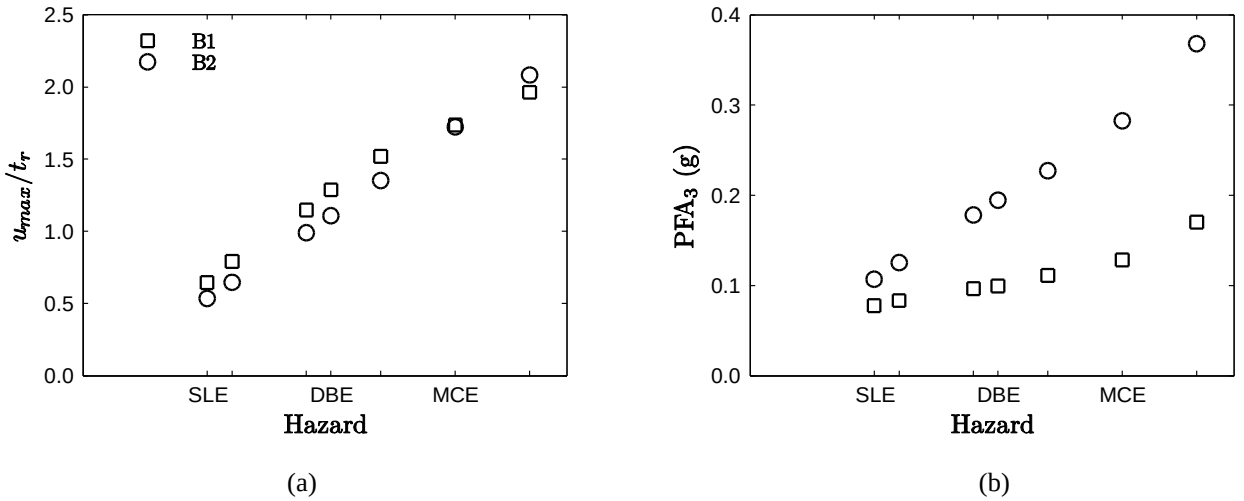

(a) (b)

Figure 8: Comparison of the model and experimental hysteresis loops for (a) isolator B1 and (b) isolator B2

Although similar values of u_{max}/t_r were observed, the values of PFA_3 were consistently greater over all hazard levels with isolator B2. In both isolators, the effect of the stiffening on the PFA_3 is visible as the rate of increase with hazard level significantly increases from 1.0 MCE to 1.2 MCE. Note that the value of PFA_3 in isolator B1 increases by only 65 % between the SLE level and the MCE level, and 120 % between SLE and 1.2 MCE. For isolator B2, the values were 164 % and 244 %, respectively. As isolator B1 experiences rollover, the force-displacement relationship becomes near-constant between u/t_r = 0.75 and u/t_r = 1.5. Thus, the response of the structure, indicated here by PFA_3, remains relatively consistent within this range of displacement amplitude.

6. DISCUSSION

In the numerical model, the two bearing designs considered with the same volume of elastomer (i.e. when considering 2 bearings of design B1, and one bearing of design B2). The results of the numerical model emphasizes the sensitivity of horizontal force-displacement relationship to the width-to-total height aspect ratio, and subsequently, the sensitivity of a base isolated structure response to the softening and stiffening due to rollover and full rollover. For the bearings considered, the smaller aspect ratio of isolator B1 (i.e. two smaller bearings in lieu of one larger bearing) was found to reduce the PFA_3 by 45 % and 55 % at the DBE and MCE, respectively, with comparable values of u_{max}/t_r as isolator B2. Note that minimal softening occurred in B2 due to the larger aspect ratio. Had B1 been compared to an isolator with a lower aspect ratio, near the point of instability (e.g. 2.5-3.0), it is expected that the difference in performance would be less pronounced.

Based on the results presented herein, there is no indication that the horizontal instability in isolator B1 at approximately u/t_r = 0.75 has had an adverse effect on the response of the structure. In most circumstances in civil engineering, a negative tangential stiffness is representative of failure or approaching failure. In conventional elastomeric bearings, horizontal instabilities often dictate the displacement capacity of the device. This is not necessarily the case for unbonded FREIs, which, through full rollover, provide a mechanism to recover the horizontal stiffness and prevent unrecoverable softening from occurring. It is postulated that unbonded FREIs can be manufactured and provide adequate isolation from ground motions with lower width-to-total height aspect ratios than previously believed. The retention of horizontal stability has determined that unbonded FREIs could be manufactured to a minimum aspect ratio of 2.5. If the condition of horizontal stability is removed, the lower-limit aspect ratio would likely be governed by rollout instability (i.e. a 90 degree rotation of the entire isolator) as shown in Figure 9.

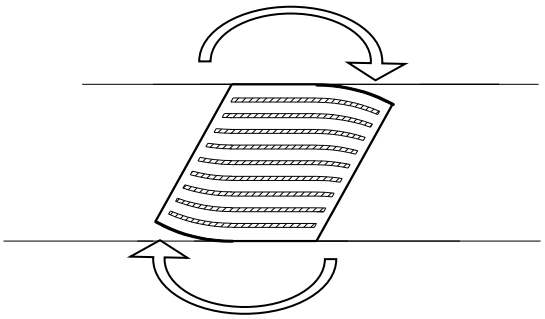

Figure 9: An unbonded FREI susceptible to rollout instability

Note that these conclusions are based on the peak isolator displacement and peak floor acceleration of the planar frame considered. The horizontal instability results in a saddle point (i.e. a local minimum). Although unlikely due to the dynamic loading conditions, the structure may rest in the saddle point after an earthquake. Thus, unstable FREIs may not behave as a self-centering system. Furthermore, isolators with lower aspect ratios are more susceptible to buckling, which was not considered in this investigation.

7. CONCLUSIONS

This paper numerically investigated the response of a structure base isolated with stable and unstable unbonded FREIs. Experimental testing of two unbonded FREIs was used to calibrate a Bouc-Wen model with a fifth-order polynomial curve to represent the characteristic softening and stiffening. The width-to-total height aspect ratio of the first isolator was half of the second isolator. In the model, the number of isolators in the former isolator was doubled to account for the reduced area. Design codes require that the horizontal force-displacement relationship of seismic base isolators maintain a positive tangential stiffness over all levels of expected displacement. For the specific devices and earthquake records considered in this paper, the results indicate that the horizontal instability did not result in any adverse effects in the response of the structure. It was found that the unstable isolator had a considerably lower peak floor acceleration than the stable isolator, and approximately equal peak isolator displacement at the hazard levels considered. Note that the softening due to rollover was limited in the stable isolator considered in this study as a result of its relatively larger aspect ratio. A substantial improvement in isolation efficiency would be expected if a lower aspect ratio had been selected, while still retaining horizontal stability.

The condition of horizontal stability has limited the width-to-total height aspect ratio of unbonded FREIs to about 2.5. It was postulated that lower aspect ratios could be allowed for unbonded FREIs, accepting and allowing horizontal instability to occur. These isolators could retain overall satisfactory, or potentially improve, performance, in comparison to designs with similar larger stable isolators. These conclusions are based on the response of the model structure. Future studies should also investigate and consider the possibility of residual displacements due to the saddle point and the susceptibility of low aspect ratio isolators to buckling.

It is recommended that similar studies be conducted considering more complex structures, ground motions with different characteristics, and with other isolator designs and width-to-total height aspect ratios.

ACKNOWLEDGEMENTS

Financial support for this study was provided by the McMaster University Centre for Effective Design of Structures (CEDS) funded through the Ontario Research and Development Challenge Fund (ORDCF) as well as an Early Researcher Award (ERA) grant, both of which are programs of the Ministry of Research and Innovation (MRI).

REFERENCES

AIR Worldwide. 2013. Study of Impact and the Insurance and Economic Cost of a Major Earthquake in British Columbia and Ontario/Québec. AIR Worldwide, Boston, USA.

ASCE 7-10. 2010. Minimum Design Loads for Buildings and other Structures, ASCE/SEI 7-10. American Society of Civil Engineers, New York.

Baker, J.W., Lin, T., Shahi, S.K., and Jayaram N. 2011. *New ground motion selection procedures and selected motions for the PEER transportation research program*. Pacific Earthquake Engineering Research Center Report 2011-03, University of California, Berkeley, California, USA.

De Raaf, M.G.P., Tait, M.J., and Toopchi-Nezhad, H. 2011. Stability of Fiber-Reinforced Elastomeric Bearings in an Unbonded Application. Journal of Composite Materials, 45(18): 1873-1884.

Fenz, D. and Constantinou, M.C. 2008. Spherical Sliding Isolation Bearings with Adaptive Behaviour: Theory. Earthquake Engineering and Structural Dynamics, 37(2):163-183.

Kelly JM. 1999. Analysis of Fiber-reinforced Elastomeric Isolators. Journal of Seismology and Earthquake Engineering, 2(1): 19-34.

Kelly, J.M. and Konstantinidis, D. 2007. Low-cost Seismic Isolators for Housing in Highly-seismic Developing Countries. 10th World Conference on Seismic Isolation, Energy Dissipation and Active Vibrations Control of Structures, Istanbul, Turkey.

Kelly, J.M. and Konstantinidis, D. 2011. Mechanics of Rubber Bearings for Seismic and Vibration Isolation. John Wiley & Sons, Chichester UK.

Love, J.S., Tait, M.J. and Toopchi-Nezhad, H. 2011. A hybrid structural control system using a tuned liquid damper to reduce the wind induced motion of a base isolated structure. Engineering Structures, 33(1): 738-746.

NBCC. 2010. National Building Code of Canada 2010. Institute for Research in Construction, National Research Council of Canada: Ottawa, Ontario, Canada.

OpenSees. 2013. Open System for Earthquake Engineering Simulation. Pacific Earthquake Engineering Research Center, University of California, Berkeley, California, USA.

Russo, G., Pauletta, M., and Cortesia, A. 2013. A Study on Experimental Shear Behavior of Fiber-Reinforced Elastomeric Isolators with Various Fiber Layouts, Elastomers and Aging Conditions. Engineering Structures, 52:422–433.

Taghavi, S., and Miranda, E. 2003. Response Assessment of Nonstructural Building Elements, Pacific Earthquake Engineering Research Center Report 2003/05. University of California, Berkeley, California, USA.

Toopchi-Nezhad, H., Tait, M.J., and Drysdale, R.G. 2008. Testing and Modeling of Square Carbon Fiber-reinforced Elastomeric Seismic Isolators. Structural Control and Health Monitoring, 15(6):876-900.

Toopchi-Nezhad, H., Tait, M.J. and Drysdale, R.G., 2009a. Shake table study on an ordinary low-rise building seismically isolated with SU-FREIs (stable unbonded-fiber reinforced elastomeric isolators). Earthquake Engineering & Structural Dynamics, 38(11): 1335-1357.

Toopchi-Nezhad, H., Tait, M.J. and Drysdale, R.G., 2009b. Simplified analysis of a low-rise building seismically isolated with stable unbonded fiber reinforced elastomeric isolators. Canadian Journal of Civil Engineering, 36(7): 1182-1194.

Tsai, C.S., Chiang, T.C., and Chen, B.J. 2003. Finite element formulations and theoretical study for variable curvature friction pendulum system. Engineering Structures, 25(14): 1719-1730.

Van Engelen, N.C., Tait, M.J., and Konstantinidis, D. 2014. Model of the Shear Behavior of Unbonded Fiber-Reinforced Elastomeric Isolators. Journal of Structural Engineering, 04014169.

Van Engelen, N.C., Tait, M.J. and Konstantinidis, D. 2015a. Partially bonded Fiber-Reinforced Elastomeric Isolators. Structural Control and Health Monitoring, 22(3): 417-432.

Van Engelen, N.C., Konstantinidis, D. and Tait, M.J. 2015b. Structural and Nonstructural performance of a seismically isolated building using stable unbonded fiber-reinforced elastomeric isolators. Earthquake Engineering and Structural Dynamics.